Nanocomposite-Strengthened Dissolving Microneedles for Improved Transdermal Delivery to Human Skin

DOI: 10.1002/adhm.((please add manuscript number))

Nanocomposite Strengthened Dissolving Microneedles for Improved Transdermal Delivery to Human Skin**

*By Li Yan, Anthony P Raphael, Xiaoyue Zhu, Beilei Wang, Wei Chen, Tao Tang, Yan Deng, Himanshu J Sant, Guangyu Zhu, Kwong Wai Choy, Bruce K Gale, Tarl W Prow, and Xianfeng Chen**

[*] Prof. Xianfeng Chen
Center of Super-Diamond and Advanced Films (COSDAF) and Department of Physics and Materials Science
City University of Hong Kong
Hong Kong SAR
E-mail: xianfeng.chen@cityu.edu.hk
Li Yan, Xiaoyue Zhu, Wei Chen
Center of Super-Diamond and Advanced Films (COSDAF) and Department of Physics and Materials Science
City University of Hong Kong
Hong Kong SAR
Dr. Anthony P Raphael, Dr. Tarl W Prow
Dermatology Research Centre
School of Medicine
The University of Queensland
Princess Alexandra Hospital, Brisbane,
Australia
Beilei Wang, Prof. Guangyu Zhu
Department of Chemistry and Biology
City University of Hong Kong
Hong Kong SAR
Dr. Himanshu J Sant, Prof. Bruce K Gale
State of Utah Center of Excellence for biomedical Microfluidics
Departments of Bioengineering and Mechanical Engineering
University of Utah
Salt Lake City, UT 84112,
USA
Dr. Tao Tang, Yan Deng, Prof. Richard Choy
Department of Obstetrics & Gynaecology
The Chinese University of Hong Kong
Hong Kong SAR
CUHK Shenzhen Research Institute, Shenzhen, China

Keywords: Transdermal delivery; vaccine delivery; nanocomposite; polymeric material; biomedical applications

ABSTRACT:

Delivery of drugs and biomolecules into skin has significant advantages. To achieve this, herein, we report a nanomaterial strengthened dissolving microneedle patch for transdermal delivery. The patch comprises thousands of microneedles which are composed of dissolving polymers, nanomaterials and drug/biomolecules in their interior. With the addition of nanomaterials, the mechanical property of generally weak dissolving polymers can be dramatically improved without sacrificing dissolution rate within skin. In our experiments, as a test case, we incorporated layered double hydroxides (LDH) nanoparticles into sodium carboxymethylcellulose (CMC) to form a nanocomposite. The results show that, by adding 5 wt% of LDH nanoparticles into CMC, the elastic modulus of the polymer increases from 0.993±0.065 GPa to 2.878±0.123 GPa, which is comparable to that of engineering plastics (e.g., 2.0-2.6 GPa for polycarbonate). Small and densely packed CMC-LDH microneedles penetrate human and pig skin more reliably than pure CMC ones and attractively the nanocomposite strengthened microneedles dissolve in skin and release payload within only 1 minute. Finally, we tested the application of using our nanocomposite strengthened microneedle arrays for *in vivo* vaccine delivery and the results showed that significantly stronger antibody response could be induced when compared with that generated by subcutaneous injection. These data suggest that nanomaterials could be useful for fabricating densely packed and small polymer microneedles that have robust mechanical properties and rapid dissolution rate and therefore potential use in clinical applications.

1. Introduction

Microneedles are tiny projections of micrometer dimensions and have the capability of delivering drugs and biomolecules to skin.[1-5] This transdermal delivery platform has many advantages over conventional subcutaneous and intramuscular injection by needle and syringe. First, there is no or minimal pain, cross-infection and needle stick injuries.[6-8]

Second, microneedle can be designed to target specific layer of skin. Third, there is potential for self-administration. Last but not least, it can be used when there is a significant first-pass effect of the liver that can prematurely metabolize drugs.[9] Microneedle arrays are usually made of silicon, metals and polymers.[10] Among them, polymer microneedle arrays are increasingly attractive because they are expected to be less expensive to mass produce than silicon or metal arrays and safer during application. Drugs and biomolecules can be incorporated into the interior of microneedles themselves when using dissolving polymers.[8,11] During application, the polymer structure rapidly dissolves in skin, thereby releasing the drug and biomolecules, so there is no sharp waste.

Despite their promising features, dissolvable polymers generally have very weak mechanical properties. The need for combination of biocompatibility, robust mechanical properties and rapid dissolution rate severely limits the choice of polymer. Polyvinylpyrrolidone (PVP)[1,8,11] and carboxymethylcellulose sodium salt (CMC)[7,12] are commonly reported for making dissolving polymer microneedles. For example, PVP microneedles were fabricated by either *in-situ* polymerization of monomers under UV conditions (using a 100 W UV lamp) or heating at 80 °C for 24 hours.[1,8,11] These harsh conditions may seriously limit the incorporation of drug and biomolecules that are temperature or UV sensitive. On the other hand, CMC microneedles can be fabricated at room temperature, but CMC has weak mechanical properties. For example, the elastic modulus of CMC is only around 1 GPa.[12] It is expected that the bioresorbable polymer microneedle size needs to be relatively large to reliably pierce human skin.[12] This would apparently constrain the density of microneedles on an array. However, recent study shows that small (base diameter or width < 40 μm) and densely packed microneedles (over 10,000 microneedles per cm^2) may lead to significantly enhanced vaccine efficacy when compared to large and sparsely packed ones.[13,14] In addition, small microneedles can be easily dried during

fabrication and dissolve rapidly in skin during application. Therefore, improving the mechanical properties of dissolving polymer microneedles could be beneficial in terms of drug efficacy and design flexibility as well as ease in fabrication and rapid dissolution in the skin.

To achieve this, we hypothesize that the use of reinforcing nanofillers will result in an advanced biomedical material that can make enhanced dissolving polymer microneedles that are mechanically more robust, while retaining the capacity to rapidly dissolve. Layered double hydroxide (LDH) nanoparticles have been commonly used to reinforce a variety of polymers.[15] For example, by adding only 1 wt% of LDH nanoparticles into nylon 6, the elastic modulus of the composite increases 100% in comparison with that of pure nylon 6 polymer.[16] Therefore, in this paper, we have examined the potential for LDH nanoparticles to enhance the mechanical strength of CMC cast in microneedle arrays for potential drug and biomolecule delivery. We are the first to report the use of nanomaterials to improve the mechanical characteristics of dissolving microneedle arrays for transdermal delivery.

2. Results

2.1. Characterization of Mg_2Al-Cl-LDH Nanoparticles

We firstly prepared Mg_2Al-Cl-LDH nanoparticles with a mean size of 80 nm and zeta potential of +40 mV in aqueous and buffer-free solution (**Figure 1**a-c). The as-prepared aqueous suspension contained well suspended LDH nanoparticle without aggregation (Figure 1a-b). XRD pattern shows the typical feature of Mg_2Al-Cl-LDH nanoparticles (Figure 1d). Diffraction peaks shown in the XRD pattern of pristine LDH nanoparticles correspond to the (003), (006) and (009) plane reflections of LDH.

2.2. Mechanical Properties of CMC and CMC-LDH Nanocomposite

We incorporated varying amounts of LDH into 2 wt% CMC aqueous solution to test the strengthening effect of LDH nanoparticles on the mechanical properties of CMC. After the samples were dried, nanoindentation was used to measure their elastic modulus and hardness. **Figure 2**a shows typical load–displacement curves of CMC polymer with different concentrations of LDH nanoparticles. The nanoindentation cycle consists of three periods: loading-holding-unloading. Loading forces were increased at constant velocity and the nanoindenter tip sank into materials during the loading period, which contributed to both elastic and plastic deformation. Strong materials require a high force to achieve the same penetration depth during the loading period.[16] As we can observe from Figure 2a, much greater load is required for penetration of the same depth as LDH nanoparticle concentration increases from 0 wt% to 2, 5 and 10 wt% (relative to the mass of CMC in the samples). Apparently, adding LDH nanoparticles into CMC can significantly enhance its resistance to indentation and make CMC-LDH composite much stronger than pure CMC. Figure 2b and Figure 2c show the elastic modulus and hardness of polymers, respectively, calculated from unloading. The elastic modulus of pure CMC is 0.993±0.065 GPa. The elastic modulus of 2 wt% of LDH loaded CMC increased to 1.489±0.036 GPa. With LDH concentration increased to 5 wt%, the elastic modulus reaches 2.878±0.123 GPa. The elastic modulus increased to 290% of that of pure CMC polymer when 5 wt% of LDH nanoparticles were added to CMC ($p < 0.001$). When the LDH concentration was increased to 10 wt%, the elastic modulus of the nanocomposite started to decrease. It should be noted that the hardness of pure CMC polymer is 0.067±0.001 GPa. The addition of LDH nanoparticles to CMC increased the hardness of the composite material to 0.080±0.001 GPa, 0.111±0.004 GPa and 0.118±0.001 GPa for CMC composites with 2 wt%, 5 wt% and 10 wt% of LDH nanoparticles, respectively.

Based on these results we chose the CMC composite with 5 wt% LDH nanoparticles as the starting material for preparing microneedle arrays. Since centrifugation (3000 × g for 10 minutes) was used to force the viscous polymer solution to fill in the tiny cavity of a microneedle PDMS mold, the concentration of CMC aqueous solution was increased to 5 wt% to avoid unequal LDH nanoparticle distribution within the centrifuged microneedles. When 5 wt% LDH (relative to the mass of CMC) was added to the 5wt% CMC solution followed by centrifugation at 4000 × g for 10 minutes, negligible amount of LDH nanoparticles was sedimented by simply observing the mixture solution. The bottom layer of the solution was discarded and supernatant was used for nanoindentation measurements. The results show that the elastic modulus of 5 wt% CMC/5 wt% LDH was 2.486±0.186 GPa. The value is slightly lower than the highest elastic modulus of the sample dried from the solution of 2 wt% CMC incorporating with 5 wt% LDH, but it is still much better than that of pure CMC ($p < 0.001$). The suspension of 5 wt% CMC/5 wt% LDH was then used for fabricating microneedles.

2.3 Characterization of CMC-LDH Nanocomposite Microneedle Patches

The validation of the hypothesis that incorporation of LDH nanoparticles into CMC could significantly increase the mechanical properties of the polymer supported the use of this nanofiller-improved polymer to fabricate and test microneedle arrays. **Figure 3**a and Figure 3b are representative SEM images of silicon microneedle male molds used to prepare PDMS female molds for polymer microneedle fabrication. The height and density of silicon microneedles are 218 μm and 11,900 projections cm^{-2}, respectively. Figure 3c and Figure 3d show typical SEM images of our dissolving polymer microneedles. The polymer microneedles had uniform morphology and geometry. The microneedles were pyramidal in shape and the tip radius is below 500 nm. The length of these fabricated polymer projections is 165±3 μm (n=20 projections). This indicates a 24±1% reduction in length in comparison

with that of the microneedles of the male mold. This decrease is mainly due to the contraction and solidification of CMC based composite materials during drying.

2.4. Confocal Microscopy Study of the Penetration and Payload Delivery of Nanocomposite Microneedle Patches in Human and Pig Skin

Once nanocomposite microneedle patches were successfully made, the next key question was whether these microneedles can reliably penetrate stratum corneum and delivery payload to skin? To perform this study, FITC-Dextran was simply mixed with CMC-LDH nanoparticle solution as a viewable drug and biomolecule surrogate and then cast onto the tips of microneedles and then we tested nanofiller composite microneedle penetration in excised pig and human skin. To determine whether the microneedles can uniformly penetrate skin, reflectance confocal microscopy (RCM) was used to image both the treated pig skin and human skin (representative images shown in **Figure 4**a-d). Nanocomposite microneedles applied to *pig* skin resulted in successful breaching of the stratum corneum and uniform penetration within the skin across the array (Figure 4a). The penetration depth analyzed from the RCM images was 71±7 μm (n = 40 projections). These results differed from what was observed for the CMC only microneedles where the penetration was not uniform (Figure 4b). The center area shows penetration but no penetration holes are able to be clearly observed in the rest area. The depth of the penetration in the center area was found to be 46±12 μm (n = 40 projections, $p < 0.001$ between CMC and CMC-LDH microneedles penetration in pig skin). The nanocomposite microneedles also resulted in successful breaching and penetration into *human* skin (Figure 4c) with a depth of 64±9 μm (n = 40 projections). The CMC only microneedles resulted in indents on the skin surface with minimal penetration of 39±8 μm (n = 40 projections, $p < 0.001$ between CMC and CMC-LDH microneedle penetration in human skin) (Figure 4d). Besides achieving apparent deeper penetration depth in both pig and human skin, CMC-LDH nanocomposite microneedles can be more reliable on successful application

while CMC microneedles result in inconsistent penetration across the array, due to the microneedles bending on skin surface sometimes.

The RCM samples were then imaged using laser scanning confocal microscopy (LSCM) to determine payload dissolution and diffusion within the skin (representative images shown in **Figure 5**a-h). For pure CMC microneedle applied skin samples, the images were selected from the area where penetration of microneedles into skin was achieved. The delivery sites are clearly observed from the top view of the skin samples (Figure 5a, 5c, 5e and 5g), which further confirms the polymer microneedles are able to pierce stratum corneum. For some delivery sites, it is obvious to see the holes created by the microneedle penetration. The corresponding 3-D images (Figure 5b, 5d, 5f and 5h) clearly show that the FITC payload was delivered vertically to certain depths beneath the skin surface. In a number of delivery sites, it is even possible to see that the delivery payload started to diffuse a lot within the skin after only 5 minutes. Collectively, Figure 5 demonstrates that the microneedles were capable of piercing stratum corneum followed by dissolving in the skin and delivering the FITC payload to the thin layer beneath the skin surface.

Now we have confirmed that the CMC-LDH nanocomposite microneedles can reliably penetrate skin and deliver the payload into skin. Compared with CMC microneedles, the nanomaterial strengthened microneedles result in more consistent penetration within the skin cross the whole patch area. Another key question is whether these mechanically strengthened microneedles can still rapidly dissolve in skin? To investigate this, we observed the microneedles before application in skin and at 1, 2 and 5 minutes after skin penetration. The results are shown in **Figure 6**. The figure shows the merged fluorescence and reflectance confocal microscopy images of microneedles before and after being applied to skin. Before application, the fluorescent payload can be clearly seen in green throughout the shaft of the microneedles (Figure 6a). No fluorescence signal could be detected at the base of the array,

which has the added benefit of reducing cost through conserving drug molecules to the microneedles only and therefore reducing drug wastage during delivery. Because of this, in our experiments, minimal fluorescence was seen on the surface between the microneedles due to the payload being cast within the projections instead of 'wasted' in the backing layer of the microneedles. After skin application, it can be seen that almost all of the microneedles are dissolved in the skin after only 1 minute.

2.5. In vivo Delivery of Antigen to Skin and Successful Immunization of Mice

Having confirmed that our nanocomposite microneedles can robustly penetrate, quickly deliver payload to human and pig skin and target specific skin layers, next we test the application of the nanocomposite microneedle arrays for vaccine delivery. We fabricated CMC and CMC-LDH microneedle arrays with 10 and 1.65 μg of ovalbumin (OVA) protein, respectively. Pure CMC polymer microneedle arrays were used as a control in the experiment. Mice were anesthetized and a single microneedle patch was applied to each ear, therefore 2 microneedle patches were used for each mouse. As a positive control, we subcutaneously injected 20μg of OVA protein to mice. The induced antibody titers of mice are shown in **Figure 7**. From the figure, the following can be observed. At 14 days after primary immunization, subcutaneous (SC) injection of 20 μg of OVA protein induced negligible immune response compared with that of unimmunized mice. In great contrast, both CMC and CMC-LDH microneedle vaccination led to great immune response indicated by the high antibody titer shown in Figure 7a. The antibody titers between the two microneedle immunized groups do not show statistical difference ($p > 0.1$). If we compare the standard error of the mean of the two microneedle groups, it is easy to find that the antibody titers generated by CMC-LDH microneedle patch vaccination are more consistent than those induced by CMC microneedle immunization.

The mice were then boosted at 17 days after primary immunization and sera were collected at 21 days after the boost (38 days after primary vaccination). From Figure 7b, it can be seen that, after boost, SC injection of 20 μg of OVA protein led to reasonably high antibody titers, although still much lower than those induced by microneedle vaccination ($p < 0.001$). The other finding is that, after boost, CMC-LDH microneedle arrays containing 3.3 μg of OVA protein led to stronger immune response than that induced by pure CMC microneedle patches with 20 μg of OVA protein ($p < 0.001$).

3. Discussion

In this paper, we hypothesized that the LDH nanoparticles could enhance the mechanical properties of CMC microneedles and thereby improve transdermal delivery. We chose CMC because it had often been used as a material in dissolving microneedles[7,12] in the literature, but the elastic modulus of CMC is only 1 GPa[12], which potentially limits the successful application of CMC microneedles in transdermal drug and biomolecule delivery for humans, particularly when one needs to fabricate densely packed microneedles for certain needs. LDH nanoparticles were selected to increase the mechanical strength of CMC because of their high biocompatibility, high aspect ratio (lateral size over thickness), low cost and previous use in enhancing mechanical strength in polymers.[15-17] Furthermore, CMC is negatively charged in solution and may well be incorporated into the internal layers of LDH nanoparticles and help disperse LDH nanoparticles uniformly. Consistent dispersion is a crucial challenge when formulating nanofillers to mechanically strengthen polymers as better dispersion of nanomaterials/fillers leads to enhanced mechanical properties.[15] The mechanical strength of CMC was greatly enhanced by adding LDH nanoparticles. The elastic modulus of our CMC-LDH composite microneedles is comparable to that of engineering plastics, e.g. 2–4 GPa for nylon and 2.0-2.6 GPa for polycarbonate. This improvement has the capacity to increase the flexibility of drug and molecule formulations that can be incorporated

into dissolving microneedle arrays. It is expected that the addition of drug and molecules, composed primarily of proteins and salts, will worsen the mechanical properties of the structural polymer in a concentration dependent manner. The addition of reinforcing nanofillers could help to curb that effect such that the final microneedle array remains useful for animal and human applications.

Our fabrication process was operated at room temperature (23 °C). Lowering the temperature to optimize the stability of the drugs and molecules could be explored using this casting technique. The entire fabrication process required no heating, UV illumination or any other harsh conditions or treatments and therefore our technique is suitable for incorporating delicate drugs and biomolecules into microneedles for subsequent transdermal delivery. The enhanced mechanical properties of the CMC-LDH composite microneedles successfully pierced pig and human skin to deliver a FITC-labeled dextran payload. Importantly, the nanoparticle strengthened polymer microneedles retained the capacity to dissolve quickly, within only 1 minute. Quick dissolution within skin is crucial for a short administration time. For comparison, in a previous report, methacrylic acid (MAA) was copolymerized with vinyl pyrollidone (VP) to form poly(vinylpyrrolidone-co-methacrylic acid) (PVP-MAA) to improve the mechanical strength of the fabricated microneedles. However, with the addition of MAA, the dissolution rate of the microneedles greatly slowed. For example, PVP-MAA microneedles (25% MAA) need 2 hours to dissolve within porcine skin while at the same size pure PVP microneedles dissolve within 15 minutes.[8]

Skin contains abundant of immune cells and the density of these cells is much high than that in subcutaneous tissue and muscle to which vaccines are usually delivered by needle and syringe injection. Therefore, if we can deliver vaccines to the skin layers, their efficacy should be greatly enhanced. Although it is possible to use conventional needle and syringe to achieve intradermal injection for delivering vaccine to the skin, it is technically challenge to perform

because the skin is very thin. To achieve reliable skin delivery, many approaches such as liquid jet injection, biolistic microparticle injection, thermal or laser assisted delivery and microneedles have been developed. [18] When these approaches were tested for vaccine delivery to skin and compared with conventional intramuscular (IM) or SC injection, it was found that the vaccine efficacy was dramatically improved. [19-22] To test whether our nanocomposite strengthened microneedle arrays can pierce skin and deliver payload to the targeted skin layers, we investigated the penetration and payload delivery by RCM and LSCM. The results confirmed that the composite microneedles successfully penetrated stratum corneum and delivered the FITC-labeled dextran payload up to around 64±9 μm below the human skin surface. The human epidermis layer contains high density of APCs and its thickness, using human forearm dorsal epidermis as an example, is 61.3±11.0 μm.[23] This means that most of the payload was delivered within the target layer.

Once demonstrating that the nanocomposite strengthened microneedle arrays could deliver payload to skin, next key question will be whether they can induce robust immune response. To investigate this, we loaded OVA protein in the microneedle arrays and performed immunization trial in mouse model. The results suggested that dissolvable pure CMC microneedle patches could induce much stronger immune response when compared with conventional efficient SC injection (generally more efficient than the commonly used intramuscular injection). Attractively, it was confirmed that the nanocomposite strengthened microneedle arrays worked even better than the pure dissolvable ones. This is in line with the findings from the penetration experiments. Because nanocomposite strengthened microneedle arrays could penetrate skin better and worked more reliably, it was apparent that the strengthened arrays should deliver more vaccine dose into skin. In other words, nanocomposite strengthened microneedle arrays were capable of increasing vaccine delivery efficiency.

Moreover, LDH nanoparticles have been widely used for efficient delivery of a range of drugs such as anticancer drug methotrexate (MTX),[24,25] low molecular weight heparin (LMWH),[26] siRNA[27-29] and plasmid DNA.[30,31] The biocompatibility and safety profiles obtained these studies will certainly help the potential use of LDH nanoparticles in our nanocomposite microneedle arrays in future clinical applications. In the meantime, it also opens the opportunity of incorporating vaccine into LDH nanoparticles for transdermal nanovaccine delivery. This will be very suitable for DNA and siRNA delivery because these molecules need to enter cells to be functional and their existence in nanovaccine form will greatly increase their intracellular delivery. In this case, LDH nanoparticles will play multifunctional roles including mechanical strengthening and nanovaccine carrier.

4. Conclusion

In this study, we demonstrated that LDH nanoparticles can reinforce dissolving polymer microneedles. By adding 5 wt% of LDH into CMC, the elastic modulus increases from 0.993±0.065 GPa to a maximum of 2.878±0.123 GPa ($p < 0.001$). Additionally, we successfully manufactured LDH nanoparticle-reinforced, dissolving polymer microneedles with uniform shape and size. The polymer microneedles have an extremely sharp tip with an average radius below 500 nm. The fabrication process was conducted at room temperature without the need for any harsh conditions that may degrade drugs and biomolecules. Confocal microscopy results confirmed that the nanofiller strengthened the dissolving microneedles by improving their mechanical properties to allow the microneedles to reliably pierce into pig and human skin, while pure CMC polymer microneedle were more likely to bend on the surface of skin. The composite microneedles retained the capacity to dissolve rapidly in skin within only 1 minute and released the incorporated payload. The payload distribution was highly localized within the skin. Finally, we tested the application of using our nanocomposite strengthened microneedle arrays for vaccine delivery and the results showed that significantly

stronger antibody response could be induced when compared with subcutaneous injection. Overall, this represents an important step toward dissolving microneedles that have robust mechanical properties with potential use in clinical applications.

4. Experimental Section

Preparation of Mg_2Al-LDH Nanoparticles: Mg_2Al-LDH nanoparticles were prepared according to the method described by Xu et al.[32,33] Briefly, 40 ml of 0.15 M NaOH (International Laboratory, USA) solution was mixed with 10 ml of solution containing 2.0 mmol of $MgCl_2$ (International Laboratory, USA) and 1.0 mmol of $AlCl_3$ (International Laboratory, USA) under vigorous stirring. The container was sealed and the solution was under stirring for 10 minutes. Next, the solution was centrifuged and washed once with water. The obtained slurry was dispersed in 40 ml of water and hydrothermally treated at 80 ℃ for 4 hours in an airtight container. The concentration of LDH is about 0.4 wt%. The mass of LDH was determined by weighing the LDH mass collected from suspension.

Fabrication of CMC-LDH Nanocomposites: LDH solutions with different concentrations were mixed with CMC (Mw 90,000, Sigma-Aldrich, USA) to make composite solution. Briefly, 10 ml of LDH solutions with different concentrations were mixed with 200 mg of CMC to prepare composite solution followed by placing in fume hood and drying to obtain polymer nanocomposite. The prepared nanocomposites contained 2 wt%, 5 wt% and 10 wt% LDH nanoparticles. The weight percentage is the mass ratio of LDH nanoparticles to CMC. During microneedle fabrication, CMC-LDH solution was centrifuged onto the mold at a speed of 3000 × g for 10 minutes. To mimic this process, for another batch of samples, 10 ml of solution containing 25mg LDH nanoparticles was mixed with 500 mg of CMC and the mixture was sonicated for 30 minutes. After that, the solution was centrifuged for 10 min at 4000 × g. The amount of the nanoparticles which were centrifuged to the bottom of solution

was trivial. The upper layer of solution was collected and sonicated for 30 minutes for being used to make nanoindentation samples and microneedle arrays.

Fabrication of Dissolving Polymer Microneedle Patches: Silicon microneedle arrays were used as male mold. The arrays were fabricated according to methods described in literature.[34] Briefly, a slicon wafer was diced by a diamond blade to create silicon microcolumns of required dimension and spacing. A two-step isotropic etching using a mixture of nitric acid and hydrofluoric acid was used to fabricate sharp microneedles. This silicon microneedle array male mold was washed with ethanol for 3 times and dried in air and then PDMS was slowly poured over the surface of silicon microneedle array. The silicon microneedle array male mold immersed in PDMS was placed in a fume hood for curing for 24 hours. After curing, the silicon microneedle array male mold was peeled off and the PDMS female mold was washed with water and ethanol for 3 times before casting. **Figure 8** shows the steps to manufacture a dissolving polymer microneedle patch. Figure 8-1 shows the PDMS mold. To make microneedle patches, firstly, 30 µl of LDH-CMC composite solution was added to the surface of mold (Figure 8-2). Then the mold was sealed (Figure 8-3) and centrifuged at 3000 × g for 10 minutes. After centrifugation, the solution remaining on the surface of the mold was collected by pipette and the mold was placed in a fume hood to dry for 30 minutes. During the drying period, a solid microneedle tip was fabricated (Figure 8-5). Subsequently, 40 µl of LDH-CMC composite solution was added to the surface (Figure 8-6) and the mold was sealed (Figure 8-7) and centrifuged for 10 minutes. Finally, 200 µl of LDH-CMC composite solution was added to the surface of centrifuged mold and placed in a fume hood for drying. After 8 hours, the mold was placed in a sealed desiccator. When the microneedle patch was dried completely, it was removed from the mold (Figure 8-9) and stored in a dessicator until use.

Characterization: Nanoindentation was carried by a MTS Nano Indenter XP® (MTS Cooperation, Nano Instrument Innovation Center, NT) with three-sided pyramid (Berkovich) diamond indenter. The indenter was pressed into materials with constant strain rate (0.05 1/s) from the sample surface into 2000 nm deep. The fabricated polymer microneedle patch was observed by scanning electron microscope (JEOL JSM-820 and FEG-SEM JEOL JSM-6335 F). The samples were tilted 45° for SEM.

Microneedle Application to Excised Skin: Excised pig ears were obtained from the local abattoir (Highchester Pty Ltd, Gleneagle, Australia). The ventral side of the ear was lightly shaved followed by thoroughly rinsing. The ventral skin (epidermis and dermis) was then separated from the ear (cartilage) using tweezers and scalpel. Excised human skin was obtained from abdominal plastic surgery patients. On arrival the adipose tissue was removed using a scalpel and the skin was rinsed. All patients signed an informed consent approved by the Princess Alexandra Hospital Research Committee approval no. 097/090. Skin (both pig and human) was stored at -20 ^{o}C prior to use. For microneedle application, the skin (pig or human) was thawed, rinsed, dried then pinned down taut on a covered corkboard. The tissue was stored on saline moistened gauze throughout the experiment when not in use. A microneedle array was then applied using a spring applicator for 1, 2 or 5 minutes (n = 3 per skin type). After microneedle application, the treatment area was excised with an 8 mm biopsy and the tissue fixed in 1 mL 4% formaldehyde in methanol for 1 hour. Following fixing, the tissue was removed and washed 3 times for 10 minutes in 1 mL 0.1M phosphate buffered saline. The samples were then stored at 4 ^{o}C until imaging.

Confocal Microscopy Observation of Skin after Patch Application: Reflectance confocal microscopy was done using a Vivascope® 1500 Multilaser (Lucid Inc., Rochester, NY, U.S.A). The protocol was adapted from a previously published procedure.[35] Briefly, a laser

diode was used to excite the tissue at 830 nm. ImageJ (NIH, U.S.A) was used to analyse the images. Laser scanning confocal microscopy was done using a Zeiss LSM 510 Meta (Carl Zeiss Inc., Germany). Prior to imaging the tissue was stained with Hoechst 33342, a nuclei stain. A stock solution of 10 mg/mL Hoechst 33342 in dimethyl sulfoxide was prepared. A working solution was made by a 1:1000 dilution in 0.1 M phosphate buffered saline. The tissue was incubated with the stain for 1 hour at room temperature followed by three washing steps for 10 minutes in 0.1 M phosphate buffered saline. The wavelengths used to excite the FITC-dextran and Hoechst 33342 was 488 nm and 405 nm, respectively.

Vaccination of OVA protein vaccine: Three groups of C57BL/6 female mice were vaccinated with OVA protein either by SC injection using needle and syringe (5 mice in the group), or microneedle array application (4 mice per group). Another group of four untreated mice were used as negative control. For SC injection, saline solution with 20 μg OVA protein was injected to each mouse. For microneedle array vaccination, one patch was applied to one ear of a mouse (total 2 patches for each mouse). The patches were applied to mice skin by a spring applicator and kept in place for 2 minutes. At 14 days after primary immunization, sera were collected. A boost vaccination was given at 17 days post primary vaccination and sera were collected at 21 days after the boost.

ELISA protocol: ELISA was performed as previously described. [36] Briefly, ELISA plates (Corning) were coated with 50 μg mL^{-1} of ovalbumin (Acros) in 0.1M of sodium bicarbonate buffer (Sigma) overnight at 4ºC. These coated plates were used to measure the titers of specific IgG induced. Color development was carried out using ABTS (diammonium 2,2-azino-bis(3-ethylbenzothiazoline-6-sulfonate; Sigma) as the substrate. The absorbance readings at 405 nm were then measured against control wells containing no antiserum in the reaction.

Acknowledgements

This study was funded by City University of Hong Kong (Project No. 7200247 and 9667053). We thank Prof. Andrey L Rogach, Dr. Andrei Susha and Dr. Steve Kershaw for providing research support and useful advices. We also acknowledge Mr TF Hung and Tsz Chun Lau for SEM observation.

[1] S. P. Sullivan, D. G. Koutsonanos, M. Del Pilar Martin, J. W. Lee, V. Zarnitsyn, S. O. Choi, N. Murthy, R. W. Compans, I. Skountzou, M. R. Prausnitz, *Nat. Med.* **2010***, 16*, 915.

[2] T. W. Prow, X. Chen, N. A. Prow, G. J. P. Fernando, C. S. E. Tan, A. P. Raphael, D. Chang, M. P. Ruutu, D. W. K. Jenkins, A. Pyke, M. L. Crichton, K. Raphaelli, L. Y. H. Goh, I. H. Frazer, M. S. Roberts, J. Gardner, A. A. Khromykh, A. Suhrbier, R. A. Hall, M. A. F. Kendall, *Small* **2010***, 6*, 1776.

[3] Q. Zhu, V. G. Zarnitsyn, L. Ye, Z. Wen, Y. Gao, L. Pan, I. Skountzou, H. S. Gill, M. R. Prausnitz, C. Yang, R. W. Compans, *Proc. Natl. Acad. Sci. U. S. A.* **2009***, 106*, 7968.

[4] S. Liu, M. Jin, Y. Quan, F. Kamiyama, H. Katsumi, T. Sakane, A. Yamamoto, *J. Control. Release* **2012,** *161,* 933.

[5] X. Chen, H. J. Corbett, S. R. Yukiko, A. P. Raphael, E. J. Fairmaid, T. W. Prow, L. E. Brown, G. J. P. Fernando, M. A. F. Kendall, *Adv. Funct. Mater.* **2011***, 21*, 464.

[6] S. Kaushik, A. H. Hord, D. D. Denson, D. V. McAllister, S. Smitra, M. G. Allen, M. R. Prausnitz, *Anesth. Analg.* **2001***, 92*, 502.

[7] A. P. Raphael, T. W. Prow, M. L. Crichton, X. Chen, G. J. P. Fernando, M. A. F. Kendall, *Small* **2010***, 6*, 1785.

[8] S. P. Sullivan, N. Murthy, M. R. Prausnitz, *Adv. Mater.* **2008***, 20*, 933.

[9] M.R. Prausnitz, R. Langer, *Nat. Biotechnol.* **2008**, *26*, 1261.

[10] K. Van der Maaden, W. Jiskoot, J. Bouwstra, J. Control. Release **2012,** *161*, 645.

[11] C. J. Ke, Y. J. Lin, Y. C. Hu, W. L. Chiang, K. J. Chen, W. C. Yang, H. L. Liu, C. C. Fu, H. W. Sung, *Biomaterials* **2012***, 33*, 5156.

[12] J. W. Lee, J. Park, M. R. Prausnitz, *Biomaterials* **2008***, 29*, 2113.

[13] X. Chen, G. J. P. Fernando, M. L. Crichton, C. Flaim, S. R. Yukiko, E. J. Fairmaid, H. J. Corbett, C. A. Primiero, A. B. Ansaldo, I. H. Frazer, L. E. Brown, M. A. F. Kendall, *J. Control. Release* **2011***, 152*, 349.

[14] G. J. P. Fernando, X. Chen, T. W. Prow, M. L. Crichton, E. J. Fairmaid, M. S. Roberts, I. H. Frazer, L. E. Brown, M. A. F. Kendall, *PLoS ONE.* **2010**, 5, e10266.

[15] Q. Wang, D. O'Hare, *Chem. Rev.* **2012***, 112*, 4124.

[16] H. Peng, W. C. Tjiu, L. Shen, S. Huang, C. He, T. Liu, *Compos. Sci. Technol.* **2009***, 69*, 991.

[17] K. Ladewig, M. Niebert, Z.P. Xu, P.P. Gray, G.Q.M Lu, *Biomaterials* **2010**, *31*, 1821.

[18] X. Chen, T. W. Prow, M. L. Crichton, D. W. K. Jenkins, M. S. Roberts, I. H. Frazer, G. J. P. Fernando, M. A. F. Kendall, *, J. Control. Release* **2009***, 139*, 212.

[19] P. C. DeMuth, W. F. Garcia-Beltran, M. L. Ai-Ling, P. T. Hammond, D. J. Irvine*, Adv. Funct. Mater.* **2013***, 23*, 161.

[20] P. C. DeMuth, Y. Min, B. Huang, J. A. Kramer, A. D. Miller, D. H. Barouch, P. T. Hammond, D. J. Irvine*, Nat. Mater.* **2013***, 12*, 367.

[21] G. J. P. Fernando, X. Chen, C. A. Primiero, S. R. Yukiko, E. J. Fairmaid, H. J. Corbett, I. H. Frazer, L. E. Brown, M. A. F. Kendall*, J. Control. Release* **2012***, 159*, 215.
[22] X. Chen, A. S. Kask, M. L. Crichton, C. McNeilly, S. Yukiko, L. Dong, J. O. Marshak, C. Jarrahian, G. J. P. Fernando, D. Chen, D. M. Koelle, M. A. F. Kendall*, J. Control. Release* **2010***, 148*, 327.
[23] N. Falstiejensen, E. Spaun, J. Brochnermortensen, S. Falstiejensen, *Scand. J. Clin. Lab. Invest.* **1988**, *48*, 519.
[24] J. Choy, J. Jung, J. Oh, M. Park, J. Jeong, Y. Kang, O. Han *, Biomaterials.* **2004***, 25*, 3059.
[25] J. Oh, S. Choi, G. Lee, S. Han, J. Choy, *Adv. Funct. Mater.* **2009***, 19*, 1617.
[26] Z. Gu, B. E. Rolfe, A. C. Thomas, J. H. Campbell, G. Q. Lu, Z. P. Xu *, Biomaterials.* **2011***, 32*, 7234.
[27] Y. Wong, K. Markham, Z. P. Xu, M. Chen, G. Q. (Max) Lu, P. F. Bartlett, H. M. Cooper *, Biomaterials.* **2010***, 31*, 8770.
[28] K. Ladewig, M. Niebert, Z. P. Xu, P. P. Gray, G. Q. M. Lu*, Biomaterials.* **2010***, 31*, 1821.
[29] Y. Wong, H. M. Cooper, K. Zhang, M. Chen, P. Bartlett, Z. P. Xu*, J. Colloid Interface Sci.* **2012***, 369*, 453.
[30] L. Desigaux, M. Ben Belkacem, P. Richard, J. Cellier, P. Leone, L. Cario, F. Leroux, C. Taviot-Gueho, B. Pitard*, Nano Lett.* **2006***, 6*, 199.
[31] J. Choy, S. Kwak, Y. Jeong, J. Park*, Angew. Chem. Int. Ed.* **2000***, 39*, 4042.

[32] Z. P. Xu, G. Stevenson, C. Lu, G. Q. Lu, *J. Phys. Chem. B* **2006***, 110*, 16923.
[33] Z. Xu, G. Stevenson, C. Lu, G. Lu, P. Bartlett, P. Gray, *J. Am. Chem. Soc.* **2006***, 128*, 36.
[34] R. Bhandari, S. Negi, F. Solzbacher, *Biomed. Microdevices* **2010***, 12*, 797.
[35] E. M. T. Wurm, C. Longo, C. Curchin, H. P. Soyer, T. W. Prow, G. Pellacani, *Br. J. Dermatol.* **2012**, *167*, 270.
[36] G. J. P. Fernando, T. J. Stewart, R. W. Tindle, I. H. Frazer, *J. Immunol.* **1998**, *161*, 2421.

Received: ((will be filled in by the editorial staff))
Revised: ((will be filled in by the editorial staff))
Published online on ((will be filled in by the editorial staff))

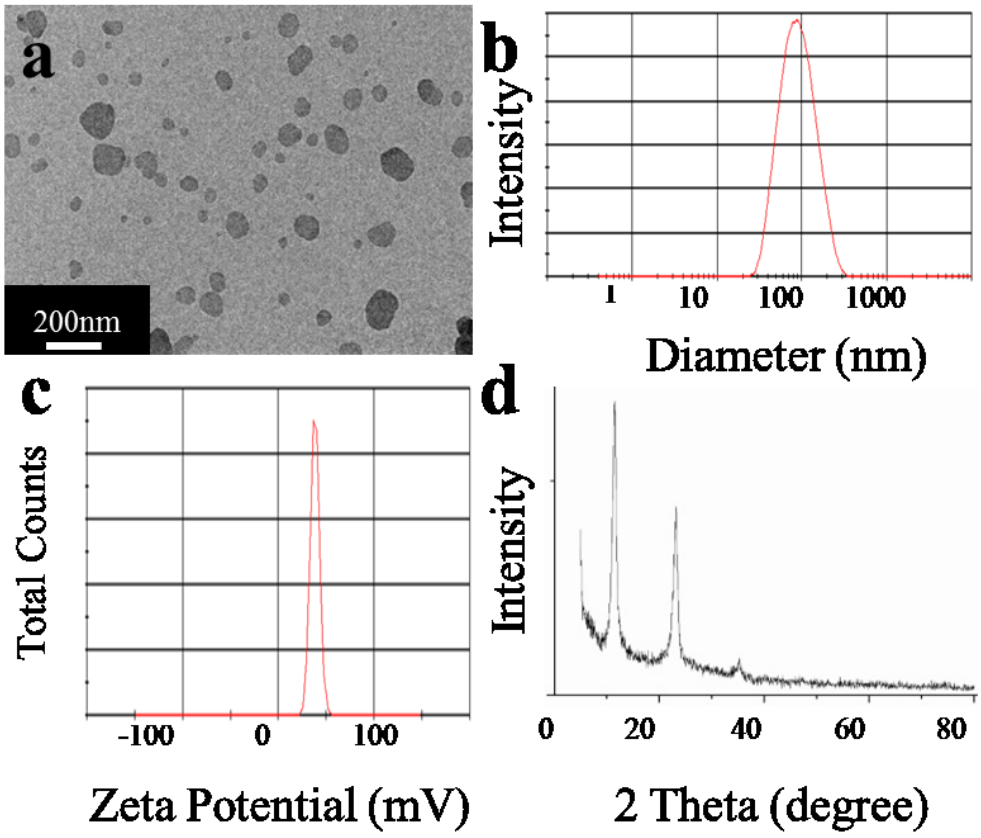

516

517 **Figure 1.** a) HRTEM image of well dispersed Mg_2Al-Cl-LDH nanoparticles. b) Particle size
518 distribution of Mg_2Al-LDH suspension. c) The zeta potential of the Mg_2Al-LDH nanoparticles in
519 aqueous and buffer-free solution. d) X-ray diffraction pattern of pristine LDH nanoparticles.

520

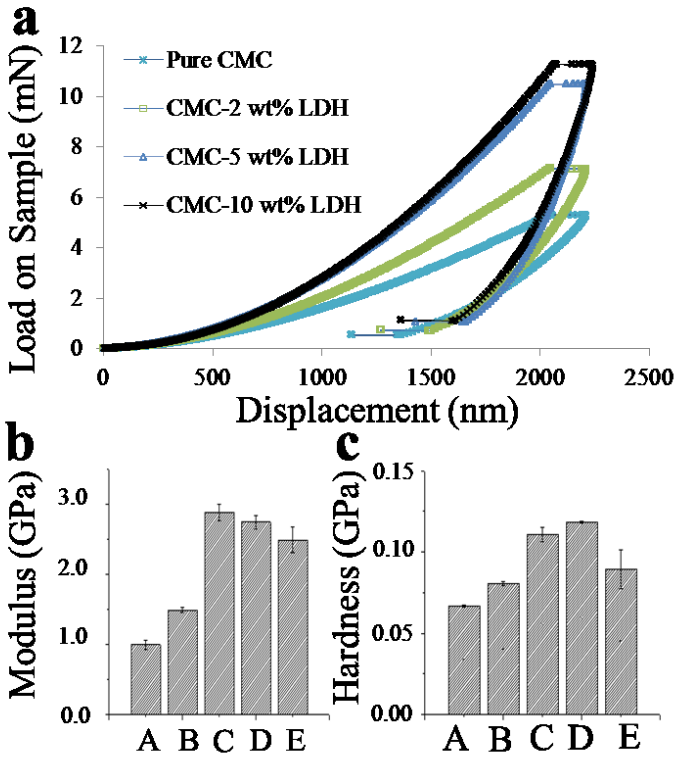

Figure 2. a) Load-displacement curves from nanoindentation. b) Elastic modulus and c) Hardness of CMC polymer films with different LDH concentrations: A-0 wt%; B-2 wt%; C-5 wt%; D-10 wt% and E-5 wt% with centrifugation.

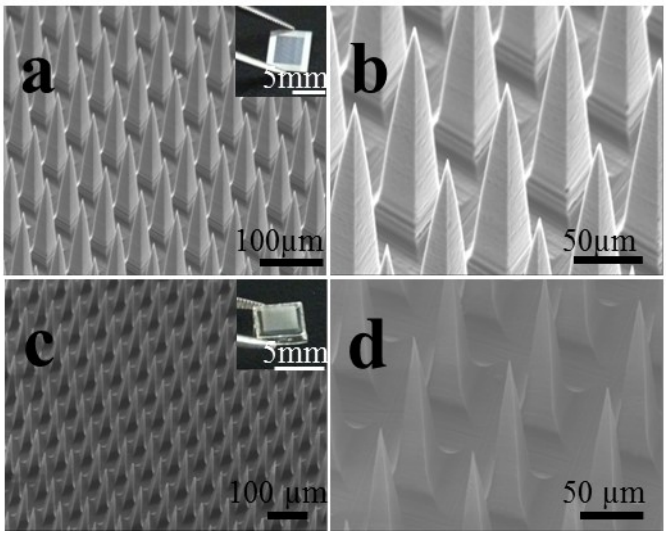

Figure 3. Scanning electron microscopy images of microneedles: a-b) Silicon microneedles array male mold (inset: digital camera image of a silicon microneedle array); c-d) Fabricated dissolving polymer microneedles (inset: digital camera image of a polymer microneedle array).

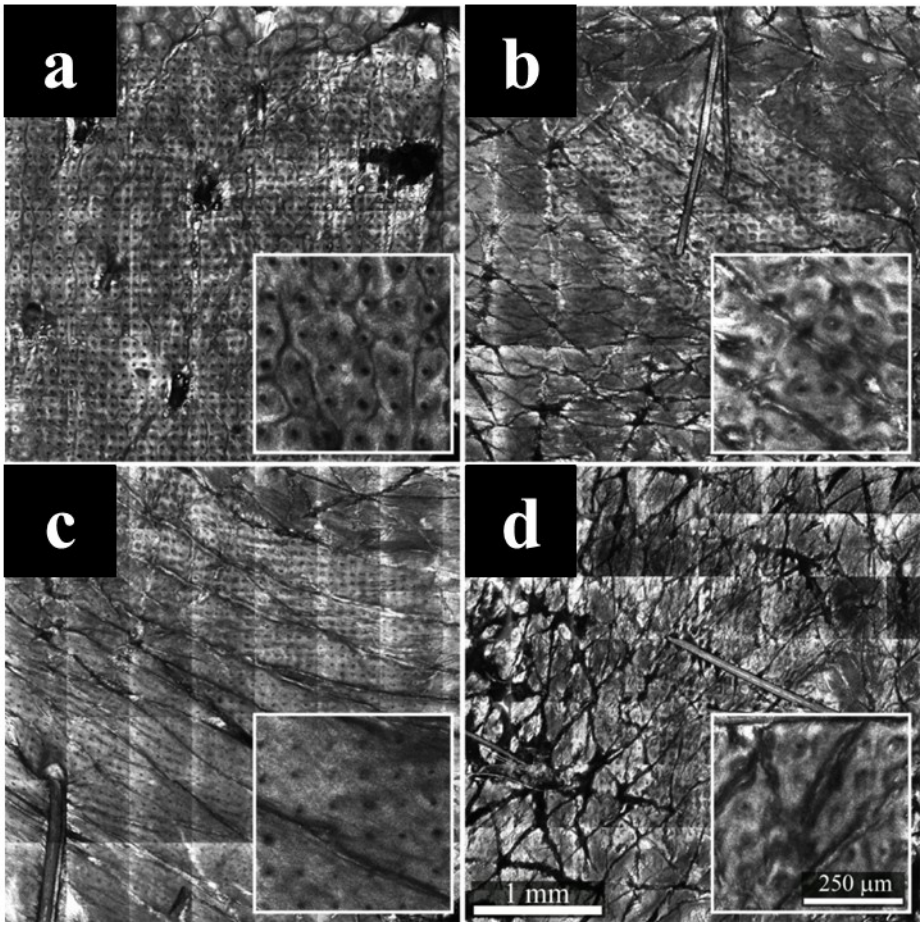

Figure 4. Reflectance confocal microscopy images of skin after 5 minutes microneedle application: a) pig skin after CMC-LDH nanocomposite microneedle application, b) pig skin after CMC microneedle application, c) human skin after CMC-LDH nanocomposite microneedle application, and d) human skin after CMC microneedle application.

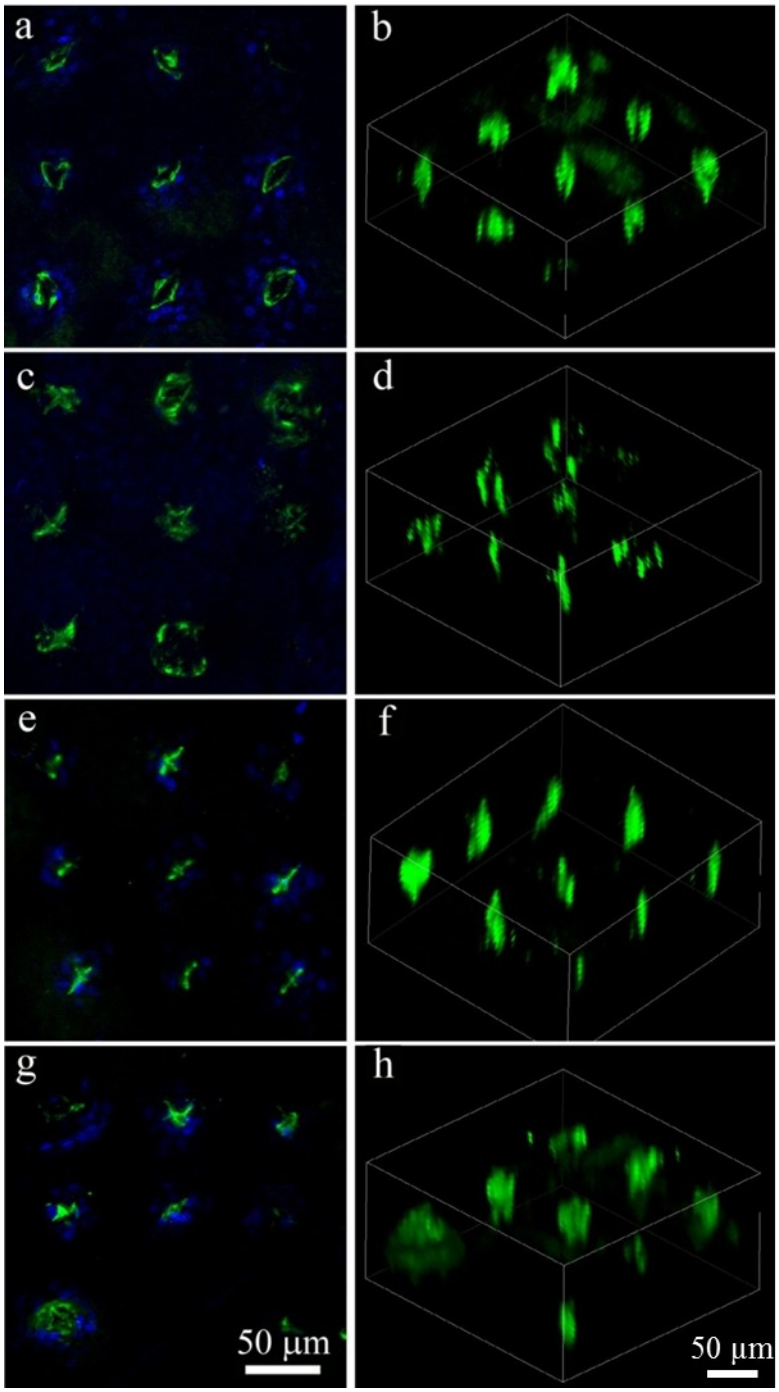

Figure 5. Laser scanning confocal microscopy images of skin after 5 minutes microneedle application: a) and b) pig skin after CMC-LDH nanocomposite microneedle application, c) and d) pig skin after CMC microneedle application, e) and f) human skin after CMC-LDH nanocomposite microneedle application, and g) and h) human skin after CMC microneedle application.

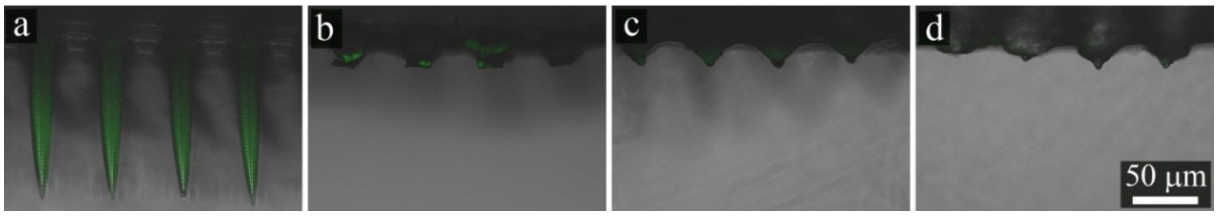

Figure 6. Merged fluorescence and reflectance confocal microscopy images of CMC-LDH nanocomposite microneedles: a) before application, b) 1 minute, c) 2 minutes and d) 5 minutes after application to pig skin.

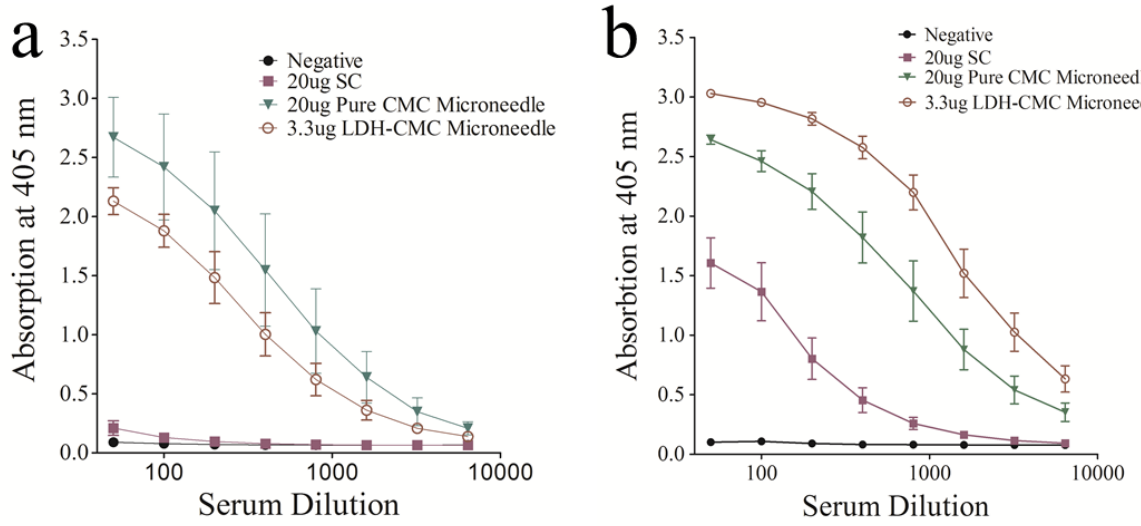

Figure 7. Total ovalbumin lgG levels at 12 and 38 days post vaccination. Five mice were subcutaneouly injected with 20 µg of OVA protein to be the positive control. Four unimmunized mice were negative control. For microneedle immunization, either pure CMC or CMC-LDH nanocomposite microneedle patches containing different amounts of OVA protein were used to vaccinate the mice. Each group has four mice. Mice were immunized at day 0 and boosted at day 17. At day 14 and 38, sera were collected and assayed for antibody titer measurements. The antibody titers at different dilutions of each group of mice were shown in the figure.

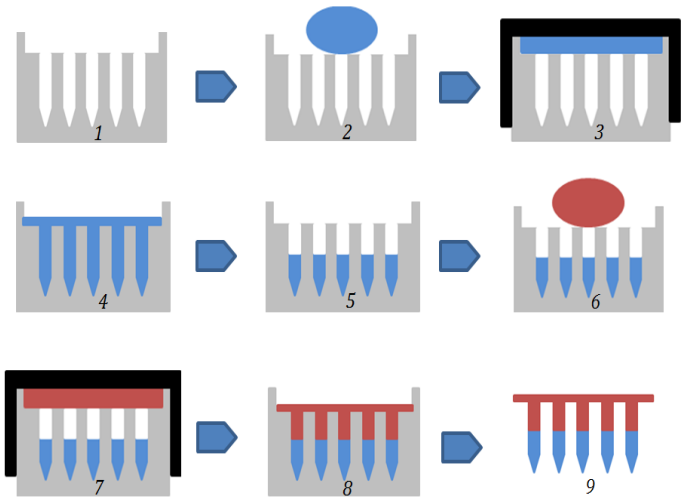

Figure 8. Steps to manufacture a dissolving nanocomposite microneedle patch.

Highly uniform nanocomposite microneedles array is fabricated under mild conditions. These very small and densely packed nanocomposite microneedles can mechanically robust enough to pierce pig/human skin, rapidly dissolve to release payload in targeted layers and induce robust immune responses.

Keywords: Transdermal delivery; vaccine delivery; nanocomposite; polymeric material; biomedical applications

Li Yan, Anthony P Raphael, Xiaoyue Zhu, Beilei Wang, Wei Chen, Tao Tang, Yan Deng, Himanshu J Sant, Guangyu Zhu, Kwong Wai Choy, Bruce K Gale, Tarl W Prow, and Xianfeng Chen*

Nanocomposite strengthened dissolving microneedles for improved transdermal delivery to human skin

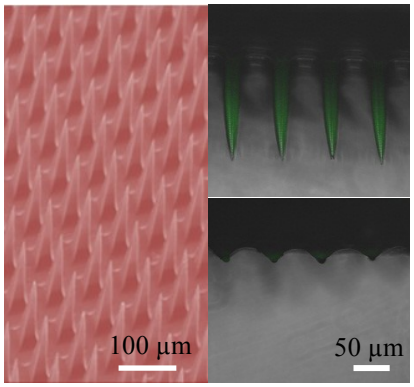

Page Headings
Left page: First Author et al.
Right page: Title of manuscript (abbreviated)